

## Anomalous selection rules and heavy-light hole beats: Stress effects in GaAs

N. H. Bonadeo,\* D. G. Steel, and R. Merlin

*The Harrison M. Randall Laboratory of Physics, and Center for Ultrafast Optical Science, The University of Michigan, Ann Arbor, Michigan 48109*

(Received 5 November 1998; revised manuscript received 14 May 1999)

Time-resolved measurements of the coherent emission due to excitons in GaAs show a polarization-dependent phase shift of the heavy-light hole exciton beating observed in the linear optical response and deviations from the usual polarization selection rules. The anomalies are ascribed to the presence of strain in the plane perpendicular to that of the light propagation. The data are in qualitative agreement with theoretical calculations based on the strain-orbit Hamiltonian and a simple harmonic model for the excitonic resonances. [S0163-1829(99)08435-0]

Since the development of ultrafast lasers, coherent transient studies have made important contributions to the understanding of the electronic and structural properties of semiconductor systems and, in particular, GaAs.<sup>1</sup> Such studies are motivated primarily by the fact that experiments with fs resolution make possible measurements of parameters difficult to obtain by other means. This methodology is also critical to the development of new ultrafast optoelectronic devices. Central to optical studies in semiconductors is the understanding of exciton dephasing and many-body interactions<sup>2,3</sup> as they play a major role in the semiconductor's resonant response. In the investigation of these effects, most studies,<sup>4,5</sup> including work on biexcitons,<sup>6</sup> and on excitation-induced dephasing,<sup>7,8</sup> rely heavily on the validity of the circularly polarized optical selection rules (CPOSR) to isolate the contributions of allowed transitions. These rules determine the spin orientation of the state created by the optical field. They follow from the  $P(S)$  character of the valence (conduction) band and the cubic  $T_D$  symmetry of GaAs. Early work on Ge, Si, and GaAs (Ref. 9) has shown, however, that the presence of strain breaking  $T_D$  symmetry can modify these rules if it leads to heavy-light hole band mixing. Since the presence of built-in stress arising from the growth and sample preparation is unavoidable, it is important to understand its effect on the optical and electronic response of the material as they relate to the outcome of coherent transient experiments.

Effects due to stress can be investigated by measuring the temporal evolution of the coherent emission induced by a single ultrashort pulse. Interesting coherent phenomena in semiconductors such as polariton beating,<sup>10</sup> Rabi flopping,<sup>11</sup> and dipole coherence beats<sup>12</sup> have been reported using this approach. In these experiments, a transient coherent optical field induces an electronic coherence aligned with the field. The induced polarization, which oscillates at the natural frequency of the resonance, gives rise to a radiated field that is phase matched in the direction of propagation of the incident field. Electronic dephasing results in a loss of coherence producing an exponential decay of the macroscopic polarization and, thus, on the radiated field. Consistent with the symmetry of GaAs, the radiated and incident fields have the same polarization. Thus, emission that is (linearly or circularly) cross polarized to the incident field is a signature of symmetry

breaking in the plane perpendicular to the light propagation. As we discuss here, this also reflects heavy-light hole mixing or, equivalently, CPOSR violation.

In this work, we report the observation of linearly cross-polarized emission that corresponds to approximately 3% of the total emitted resonant field. Our data also show that the time evolution and frequency spectrum of the cross-polarized signal differs from that of the allowed emission. In particular, the heavy-light hole beats have a  $\pi$  phase shift with respect to the beatings in the allowed configuration that we show to be a direct consequence of the sum rule dictating that the strain-induced change in the light-hole (lh) and heavy-hole (hh) oscillator strengths have different signs. The experimental results are in good agreement with calculations of the dielectric constant  $\epsilon(\omega)$ , assuming a simple harmonic oscillator model for the excitonic resonance. The stress-induced changes in  $\epsilon(\omega)$  were calculated using the strain-orbit Hamiltonian<sup>13</sup> in the presence of biaxial strain.

We use a 0.3- $\mu\text{m}$ -thick molecular-beam-epitaxy (MBE) grown GaAs bulk semiconductor sample bonded to a sapphire disk ( $c$ -axis normal) with the substrate chemically etched to allow for transmission experiments. The absorption spectrum of the sample (see Fig. 1) shows the lh and hh excitonic resonances separated by 6 meV, indicating the presence of uniaxial strain. The sample shows no significant Stokes shift in the luminescence spectrum when compared to the absorption spectrum also shown in Fig. 1.

The experimental configuration is shown in Fig. 2. The sample, placed in an optical cryostat at approximately  $T=6$  K, was excited by a single beam of 120-fs laser tuned between the lh and hh transitions (center at 1.507 eV). The

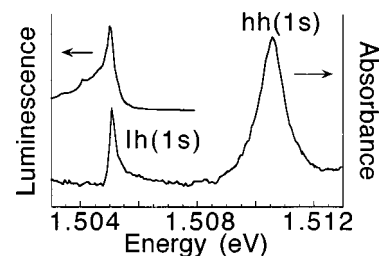


FIG. 1. Photoluminescence (upper curve) and absorption (lower curve) spectra of the bulk GaAs sample.

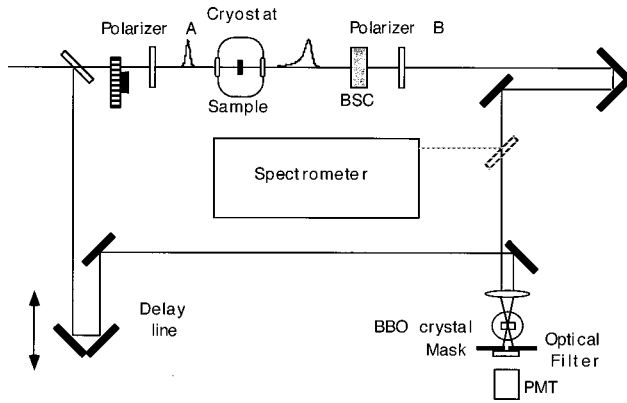


FIG. 2. Experimental configuration.

estimated exciton density was  $\sim 2 \times 10^{15} \text{ cm}^{-3}$ . The induced coherent emission following each pulse was time resolved by mixing it with a reference pulse in an efficient second-harmonic generation crystal. A metallic mask in front of the photomultiplier tube (PMT) blocked the portion of the transmitted beams that was not up-converted in the crystal and a high-pass optical filter absorbed the scattered light in the direction of the second-harmonic emission at the fundamental frequency. The intensity of the second-harmonic field as a function of the time delay between the two pulses was detected by a PMT and the generated photocurrent was measured by a lock-in amplifier. The second-harmonic field intensity as a function of time delay represents the cross-correlation function between the two field intensities. Both the excitation and reference pulse were generated by a Ti:Sapphire oscillator allowing for a pulse-width limited time resolution. The polarization of the coherent emission was analyzed by a pair of fixed polarizers. Polarizer A sets the polarization of the incoming pulse and polarizer B analyzes the emission parallel (co-polarized) or perpendicular (cross-polarized) to the excitation beam. To minimize the polarization leakage due to the optical elements in the beam path (i.e., sapphire disk, cryostat windows, etc.) we inserted a Babinet Soleil compensator (BSC) before polarizer B to compensate for the birefringence introduced by these optical elements. The polarization extinction ratio at the cross correlator at zero delay was in the range  $10^{-5}$ – $10^{-6}$  when the beam passed through the rest of the setup but not through the sample. We kept the growth direction ( $z$ ) perpendicular to the sapphire disk and parallel to the propagation of the light, and used broadband optical components to ensure a flat frequency response throughout the entire pulse bandwidth (14 meV). The spectra of the co- and cross-polarized signals were obtained by placing a mirror after polarizer B and directing the beam to a spectrometer.

Our experimental results are shown in Fig. 3. The upper plot shows the time evolution of the co- and cross-polarized coherent emission. The co-polarized signal is characterized by a nonresonant fast contribution that dominates at times close to  $t=0$  followed by a slower resonant contribution due to the hh and lh resonances. The energy difference between these excitonic states manifests itself in the beating that modulates the decay of the signal. As shown below, the phase of the beats gives information on the relative phase of the generated optical fields that is not present in the power spectrum.

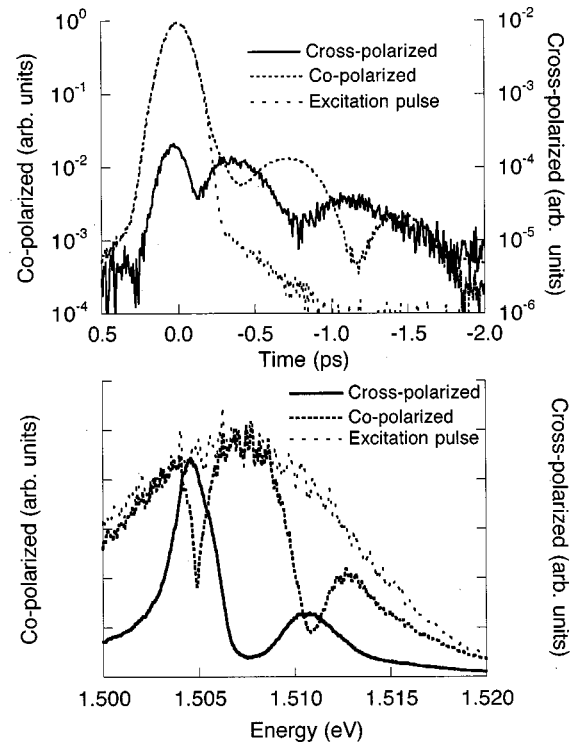


FIG. 3. Experiments. Time evolution (upper panel) and frequency spectra (lower panel) of the co-polarized and cross-polarized emission. The autocorrelation (upper panel) and the spectrum (lower panel) of the excitation pulse are also shown. For the cross-polarized data, the resolution is spectrometer limited (the slits were opened to obtain adequate signal to noise).

The cubic symmetry of GaAs predicts that there should be no coherent emission cross polarized to the incident field. That contradicts our findings in that not only does a cross-polarized signal exist, but its time evolution differs considerably from that of the co-polarized signal as seen in the solid curve of Fig. 3. The cross-polarized signal is dominated by the resonant response and the lh-hh beats have a  $\pi$  phase shift with respect to the beats in the copolarized signal. The cross correlation between the excitation pulse and the reference pulse, also shown in the plot, defines the time resolution of the experiment.

The lower plot displays the frequency spectrum of the copolarized and cross-polarized emission, and the excitation pulse. Unlike the co-polarized signal, the cross-polarized signal has a spectrum that is dominated by the resonant contribution. The cross-polarized field component accounts for about 3% of the emitted resonant field.

In the following, we show that the resonant nature of the cross-polarized signal as well as the phase shift in the lh-hh beats result from the presence of biaxial strain. There are two contributions to the strain in this sample. An unavoidable built-in strain formed during the growth process and a strain induced by mismatch of the mechanical and thermal coefficients between the GaAs layer and the supporting substrate, in this case a sapphire disk typical in low-temperature optical experiments. The mismatch, in addition, gives to the built-in stress in the GaAs layer a preferred direction (namely, perpendicular to the growth axis) which creates a uniaxial strain. The 6-meV lh-hh energy splitting observed in the ab-

sorption spectrum (Fig. 1) or, alternatively, in the temporal lh-hh beating (Fig. 2) as well as the redshift of excitonic resonances are a direct result of this strain. In general, the strain is not perfectly isotropic in the plane and thereby, it can lead to anisotropic changes in the eigenstates of the system that, in turn, modify the dipole moments of the optical transitions. This is the source of CPOSR violation.

To account for the effects of strain, we write the effective Hamiltonian of the crystal as  $\hat{H} = \hat{H}_0 + \hat{H}_{\text{SO}} + \hat{H}_e$  and consider the usual basis  $|1/2, \pm 1/2\rangle$  (split off subband),  $|3/2, \pm 1/2\rangle$  (lh), and  $|3/2, \pm 3/2\rangle$  (hh), taking the  $\hat{z}$  axis (001) as the quantization axis. The first term,  $\hat{H}_0$ , represents the non-relativistic Hamiltonian for which the three states have the same energy, the second term is the spin-orbit interaction that separates the split-off and the lh and hh bands by an amount  $\Delta E_{\text{so}}$ . The last term is the orbital-strain Hamiltonian for wave vector  $k=0$ . Assuming a diagonal strain tensor with components  $e_{xx} = e_{\perp} + \delta e$ ,  $e_{yy} = e_{\perp} - \delta e$ , and  $e_{zz} = e_{\parallel}$  where  $e_{\perp} = \alpha e_{\parallel}$  and  $\alpha$  is the Poisson's ratio for GaAs, the strain-orbit Hamiltonian can be written as

$$\hat{H}_e = -a(1-2\alpha)e_{\parallel} - 3b\left(\hat{L}_z^2 - \frac{1}{3}\hat{L}^2\right) \times (1+\alpha)e_{\parallel} - 3b\delta e(\hat{L}_x^2 - \hat{L}_y^2). \quad (1)$$

From our measurements, we know that the difference between the  $x$  and  $y$  strain components,  $2\delta e$ , is small because the cross-polarized signal is about 3% of the copolarized field component. Therefore, to lowest order in the strain the new eigenstates of the system are

$$\left|\frac{3}{2}, \pm\frac{3}{2}\right\rangle_e = \left|\frac{3}{2}, \pm\frac{3}{2}\right\rangle + \alpha_2 \left|\frac{3}{2}, \mp\frac{1}{2}\right\rangle$$

and

$$\left|\frac{3}{2}, \pm\frac{1}{2}\right\rangle_e = \left|\frac{3}{2}, \pm\frac{1}{2}\right\rangle + \frac{\alpha_1}{\sqrt{2}} \left|\frac{1}{2}, \pm\frac{1}{2}\right\rangle - \alpha_2 \left|\frac{3}{2}, \mp\frac{3}{2}\right\rangle$$

where  $\alpha_1 = [2be_{\parallel}(1+\alpha)]/\Delta E_{\text{so}}$  and  $\alpha_2 = \sqrt{3}\delta e/[2e_{\parallel}(1+\alpha)]$ . Hence, the uniaxial strain splits the lh and hh bands while the in-plane anisotropy component of the strain tensor mixes them.

We calculate the changes in the oscillator strength as a function of the unperturbed oscillator strength and the strain tensor components. The modified oscillator strength of the transitions can be written as  $f'_{i,\text{lh}} \cong f_{\text{lh}} - \delta f_{\text{so}} + \delta f_{i,\text{lh}}$ ,  $f'_{i,\text{hh}} \cong f_{\text{hh}} + \delta f_{i,\text{hh}}$  and  $f'_{\text{so}} \cong f_{\text{so}} + \delta f_{\text{so}}$  where  $f'_{i,j}$  is the oscillator strength of the  $j = \text{lh, hh}$  resonance for light polarized along the  $i = x, y$  axis. The changes in the oscillator strength are

$$\begin{aligned} \delta f_{x,\text{hh}} &= -\delta f_{y,\text{hh}} \cong f_{\text{hh}} \left(2\frac{\alpha_2}{\sqrt{3}}\right), \\ \delta f_{x,\text{lh}} &= -\delta f_{y,\text{lh}} \cong f_{\text{lh}}(-2\sqrt{3}\alpha_2), \\ \delta f_{x,\text{lh}} &= -\delta f_{x,\text{hh}}, \\ \delta f_{\text{so}} &= \alpha_{\text{I}} f_{\text{so}}. \end{aligned} \quad (2)$$

Clearly, the total oscillator strength is conserved as predicted by the sum rule. Using a simple harmonic oscillator model for the linear optical response of the exciton system, we obtain the following expressions for the dielectric response associated with the  $x$  and  $y$  axes:

$$e_i(\omega) = e_b + 4\pi\chi_{\text{res}}(\omega) + 4\pi\delta\chi_{\text{res}}(\omega)_i + \delta e_{i,b}, \quad i = x, y \quad (3)$$

where

$$\chi_{\text{res}}(\omega) = \frac{(f_{\text{lh}} - \delta f_{\text{so}})}{(\omega_{\text{lh}} - \omega) + i\gamma_{\text{lh}}} + \frac{f_{\text{hh}}}{(\omega_{\text{hh}} - \omega) + i\gamma_{\text{hh}}}$$

is a susceptibility that reflects the isotropic resonant contribution, and

$$\delta\chi_{\text{res}}(\omega)_i = \frac{\delta f_{i,\text{lh}}}{(\omega_{\text{lh}} - \omega) + i\gamma_{\text{lh}}} + \frac{\delta i_{i,\text{hh}}}{(\omega_{\text{hh}} - \omega) + i\gamma_{\text{hh}}}$$

describes the stress-induced resonant birefringence.  $e_b \sim 13$  accounts for the nonresonant contributions to the dielectric constant<sup>14</sup>  $\delta e_{i,b}$  is the stress-induced nonresonant birefringence ( $\delta e_{x,b} = -\delta e_{y,b}$ ), and  $\omega_{\text{hh}}(\omega_{\text{lh}})$  and  $\gamma_{\text{hh}}(\gamma_{\text{lh}})$  are, respectively, the resonance frequency and the damping constant of the hh (lh) resonance.

We solve Maxwell's equations inside the material to obtain the field after it propagates a distance  $d$ :

$$\begin{pmatrix} E_{\text{co}}(d, \omega) \\ E_{\text{cross}}(d, \omega) \end{pmatrix} = \begin{pmatrix} E_0(0, \omega) [\cos^2(\theta) e^{ik_x(\omega)d} + \sin^2(\theta) e^{ik_y(\omega)d}] \\ 2E_0(0, \omega) \sin(2\theta) (e^{ik_x(\omega)d} - e^{ik_y(\omega)d}) \end{pmatrix}.$$

Expanding this expression for  $|k_y(\omega) - k_x(\omega)|d \ll 1$  we obtain

$$\begin{pmatrix} E_{\text{co}}(d, \omega) \\ E_{\text{cross}}(d, \omega) \end{pmatrix} \approx E_0(0, \omega) e^{ik_x(\omega)d} \begin{pmatrix} 1 + i[k_y(\omega) - k_x(\omega)]d \sin^2(\theta) \\ 2 \sin(2\theta) i[k_x(\omega) - k_y(\omega)]d \end{pmatrix}. \quad (4)$$

Here,  $\theta$  is the angle between the polarization of the field at  $z=0$  and the  $x$  axis,  $E_0(0, \omega) = 1/2\pi \int_{-\infty}^{\infty} e^{i\omega t} [E_0(0, t)] dt$  is the field at  $z=0$ , and  $k_i(\omega) = \omega/c \sqrt{\mu e_i(\omega)}$  is the wave vector for light polarized along the  $i$  axis. The subindices ‘‘co’’ and ‘‘cross’’ indicate fields polarized parallel and perpendicular to the driving field at  $z=0$ . We note that to lowest order  $|k_y(\omega) - k_x(\omega)| \propto F(\omega) \delta e/e_{\perp}$ , where  $F(\omega)$  is an arbitrary function of  $\omega$ .

To compare our calculations with the experimental data, we numerically solve Eq. (4), obtain the spectrum, and find the cross correlation with the reference beam. We assume a Gaussian pulse profile with full width equal to 120 fs. The oscillator strength, resonance frequency, lh-hh splitting, and damping constants are taken from the absorption spectrum. Even though many parameters are involved in the numerical calculations, the qualitative features do not depend significantly on the particular set chosen, thus, no effort was made to find the best fit. The theoretical results for  $\theta = \pi/4$ , de-

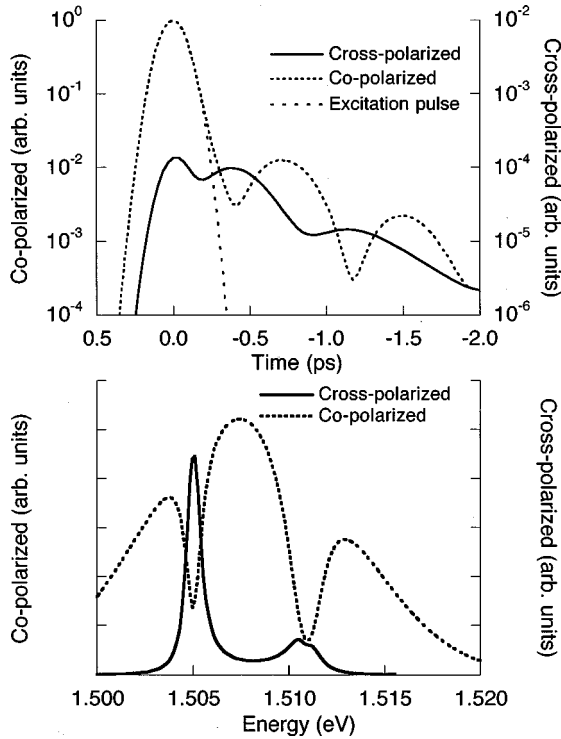


FIG. 4. Calculations that simulate the data of Fig. 3. Time evolution (upper panel) and frequency spectra (bottom panel).

picted in Fig. 4, reproduce the important features of the measurements, namely, a small cross-polarized coherent component dominated by resonant emission that shows lh-hh beating, phase shifted by  $\pi$ . This last result reflects the opposite sign of the differential oscillator strength in the  $x$  and  $y$  axes [Eq. (2)].

It is important to emphasize the fact that the angle  $\theta$  affects the amplitude, but not the overall behavior of the cross-polarized signal. Experimentally, we did not observe a strong dependence of the cross-polarized intensity on the angle between the light polarization and the crystal axes, except close to the edges of the sample. From this we infer that the orientation of the principal axes of the dielectric tensor is not uniform but fluctuates on a length scale small compared to the laser spot size of  $\sim 200 \mu\text{m}$ .

From the value of the lh-hh splitting we can estimate that of the uniaxial strain and, then, use this value, together with the measured cross- and copolarized signal strength ratio, to calculate the amount of strain anisotropy in  $x$ - $y$  plane. We are also taking into account that the signal intensity is an average over the angle  $\theta$ . The calculation yields  $e_{\parallel} \sim 6.8 \times 10^{-4}$  and the average  $\delta e \sim 3 \times 10^{-5}$ . We note that while this paper examined the strain-induced changes in the polarization in the limit of the linear optical response, at higher excitation levels, coherent exciton-exciton interactions have been predicted to significantly modify the polarization properties in these strained systems.<sup>15</sup>

We have also observed strain-induced effects in other bulk GaAs and GaAs/ $\text{Al}_x\text{Ga}_{1-x}\text{As}$  quantum well samples. Figure 5 shows data obtained in a quantum well sample consisting of 10 periods of 100-Å GaAs wells and 100-Å of  $\text{Al}_{0.3}\text{Ga}_{0.7}\text{As}$  barriers grown by MBE. The experimental conditions were the same as in the previous experiment. The data show many similarities to the data obtained in bulk

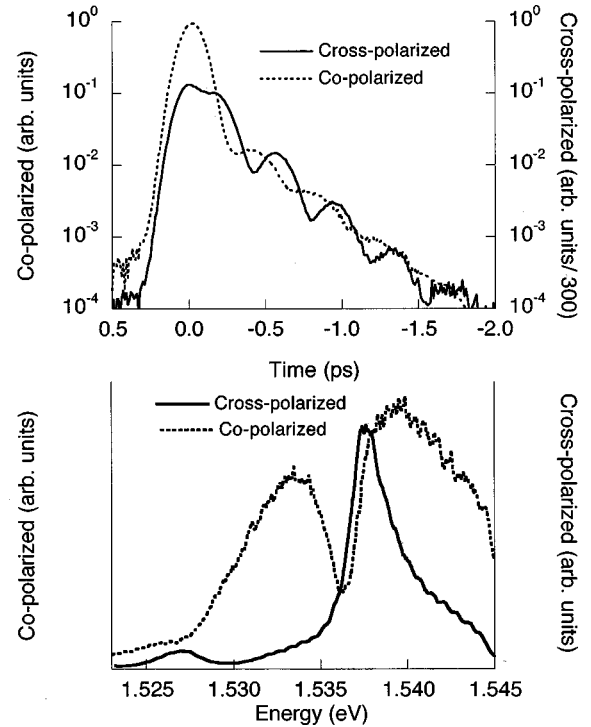


FIG. 5. Measured time evolution (upper panel) and frequency spectra (lower panel) of the co-polarized and cross-polarized emission in a quantum well sample.

GaAs. The temporal oscillations of the cross-polarized and co-polarized emission are initially  $\pi$  shifted and the cross-polarized emission spectrum has clear resonant features as expected from our model. We note, however, that the period of the cross-polarized temporal oscillations is shorter than that of the co-polarized temporal oscillations. This is also reflected in the small frequency shift in the cross-polarized spectrum with respect to the absorption resonances observed in the co-polarized emission. The physical origin of this phase shift and the difference in the period of the temporal oscillations cannot be accounted for in our model and is currently under investigation. We expect the stress-induced effects described in this work to be present in other materials and heterostructures as well, in particular those with a large lattice mismatch, which show large built-in strain in the growth plane.

Our time-domain method for estimating the strain has some advantages over the more traditional cw ellipsometry.<sup>16</sup> A simple example is when a broadband nonpolarized background scattering source such as surface roughness is present in the sample and cw experiments cannot distinguish between the scattering light and the signal. Here, our approach provides a background free determination of the resonant component because the scattered light contributes only at times close to  $t = 0$ , allowing measurements to be made away from zero delay. Another clear advantage is that we can obtain information about the relative phase of the emitted field, as discussed above, that is not present in the power spectrum. In our experiments this allowed for the measurement of the relative sign of the lh and hh oscillator's strength change, finding it consistent with the proposed biaxial induced birefringence model.

In summary, we have shown that the presence of biaxial

strain in GaAs leads to coherent emission that is cross-polarized with respect to the polarization of the excitation pulse, in disagreement with CPOSR predictions. The time evolution of the signal reveals a polarization dependent phase shift of lh-hh beats. The temporal response as well as the frequency response of the signal are in qualitative agreement with theoretical predictions based on the orbital-strain model.<sup>9</sup>

The use of time-domain techniques to measure strain should allow one to extend birefringence studies to samples in which background scattering is the limiting factor and obtain information regarding the sign of the induced changes that is not available in standard cw ellipsometry.<sup>16</sup>

This work was supported by ARO, AFSOR, and NSF through the Center for Ultrafast Optical Sciences. We would like to thank J. R. Guest for helpful discussions.

---

\*Present address: Bell Laboratories, Lucent Technologies, Holmdel, NJ 07733.

<sup>1</sup>J. Shah, *Ultrafast Processes in Semiconductors and Semiconductor Nanostructures* (Springer, Berlin, 1996).

<sup>2</sup>D. S. Chemla, S. Schmitt-Rink, and D. A. B. Miller, in *Optical Nonlinearities and Instabilities in Semiconductors*, edited by H. Haug (Academic, San Diego, 1988), p. 83.

<sup>3</sup>H. Haug and S. W. Koch, *Quantum Theory of the Optical and Electronic Properties of Semiconductors* (World Scientific, Singapore, 1993).

<sup>4</sup>S. Schmitt-Rink, D. Bennhardt, V. Heucheroth, P. Thomas, P. Haring, G. Maidorn, H. Bakker, K. Leo, D.-S. Kim, J. Shah, and K. Köhler, *Phys. Rev. B* **46**, 10 460 (1992).

<sup>5</sup>R. E. Worsley, N. J. Traynor, T. Grevatt, and T. T. Harley, *Phys. Rev. Lett.* **76**, 3224 (1996).

<sup>6</sup>K. B. Ferrio and D. G. Steel, *Phys. Rev. B* **54**, R5231 (1996).

<sup>7</sup>H. Wang, K. Ferrio, D. G. Steel, Y. Hu, R. Binder, and S. Koch,

*Phys. Rev. Lett.* **71**, 1261 (1993).

<sup>8</sup>A. E. Paul, W. Sha, S. Patkar, and A. L. Smirl, *Phys. Rev. B* **51**, 4242 (1995).

<sup>9</sup>F. H. Pollak and M. Cardona, *Phys. Rev.* **172**, 816 (1968).

<sup>10</sup>T. Mishina and Y. Masumoto, *Phys. Rev. Lett.* **71**, 2785 (1993).

<sup>11</sup>S. T. Cundiff, A. Knorr, J. Feldmann, E. O. Göbel, and H. Nickel, *Phys. Rev. Lett.* **73**, 1178 (1994).

<sup>12</sup>D. Fröhlich, A. Kulik, B. Uebbing, A. Mysyrowicz, V. Langer, H. Stoltz, and W. von der Osten, *Phys. Rev. Lett.* **67**, 2343 (1991).

<sup>13</sup>G. E. Pikus and G. L. Bir, *Fiz. Tverd. Tela (Leningrad)* **1**, 1642 (1959) [*Sov. Phys. Solid State* **1**, 1502 (1959)].

<sup>14</sup>H. C. Casey, D. D. Sell, and M. B. Panish, *Appl. Phys. Lett.* **24**, 63 (1974).

<sup>15</sup>R. Binder, *Phys. Rev. Lett.* **78**, 4466 (1997).

<sup>16</sup>R. Azzam and N. Bashara, *Ellipsometry and Polarized Light* (North-Holland, New York, 1986).